ISSN 1746-7659, England, UK
Journal of Information and Computing Science
Vol. 6, No. 3, 2011, *pp*. 234-240

A Discontinuous Galerkin Level Set Method for Compressible two Fluid Flow

Eryun Chen[1], Gaiping Zhao[2], Ailing Yang[1], Qingyi Sai[1]

[1]School of Energy and Power, University of Shanghai for Science and Technology, Shanghai 200093, China

[2]School of Medical Instrument and Food Engineering, University of Shanghai for Science and Technology, Shanghai 200093, China

(*Received June 13, 2011, accepted June 20, 2011*)

Abstract. It is a crucial problem in the studies of the fluid on numerical simulations of the interfaces movement in multi-component fluids. In the present paper, a discontinuous Galerkin method is developed to simulate two-fluid flow. A level set method is used to capturing moving interfaces and a ghost fluid method with isobaric fix is used to disposing the interfaces boundary. Several test problems of two fluid flowing is solved and the comparisons between the numerical results and exact case are performed, which indicate the effectiveness of the method.

Key words: Multi-media flow; DG method; Level Set Method; GFM

1. Introductions

Discontinuous Galerkin method was initially introduced by Reed and Hill[1] to solve linear neutron transport equations. Lesaint and Raviart[2] were the first to put this method on a firm mathematical basis. Since that time, rigorous analyses of the method are made by Johnson[3], Richter[4], and by Peterson[5], Especially Cockburn and Shu introduced an explicit, nonlinearly stable high order Runge–Kutta type time discretization[6], which makes it to be an attractive method in computational fluid dynamics(CFD)[7-8].

But as we all know, when a well established numerical method for single-medium flow is applied directly to the multi-medium flow, there can arise severe nonphysical oscillations in the vicinity of the material interface especially in the presence of shock and large density ratio[9]. As such, numerical simulation of multi-medium flow is an important interesting area in recently science computation. Especially two-fluid, where two non-mixing fluids are separated by a sharp fluid interface, find many applications in both engineering and physics[10]. The main difficulty in computing multi-medium flow is how to treat the moving medium interface. A general classification of interface methods in multi-material flows simulation divides them into Lagrangian and Eulerian[10-12]

Lagrange methods[11] use the interface particles to characterize the interface and move with the fluid in order to capture the interface movement. It has extreme precision on the interface simulation. This method can accurately track the interface evolution and can discontinuously treat no numerical dissipation, but it is hard to treat the variation of interface topological structure and complicated to develop to high dimension. Euler methods[12] are effective to treat most problems and can treat the large deformation movement, but it is unable to precisely locate the multi-component interface and is unsuitable to the numerical simulation that requires high interface position. The robust ideal method must have both their merits.

A technique coupling level set method[13] and ghost fluid method(GFM) developed[12] by Osher, Sethian and Fedkiw provides an attractive alternative for multi-medial flow simulation. Level set method is used to capture the interface position, and GFM is used to define the state variables of neighboring mesh points on the interface. At the same time, an interface entropy interpolation technique is used to capture the suitable interface boundary conditions in order to decrease possible non-physical oscillation.

In the present paper, a discontinuous Galerkin(DG) method[6-8] is developed to simulate two fluid flow. In computational, a level set method is used to capturing moving interfaces and a GFM with isobaric fix is used to disposing the interfaces boundary. Several test problems of two fluid flowing is solved and the

[1] Corresponding author. *E-mail:* chen_eryun@yahoo.com.cn

comparisons between the numerical results and exact case are performed, which indicate the effectiveness of the method.

The paper is organized as follows. We begin by describing the mathematical model in section 2 and the numerical discretisation of the Euler equations and level set function are presented in section 3, and then GFM with isobaric fix are given in section 4. Section 5 contains the associated numerical results. Finally, we sum up our conclusions in Section 6.

2. Mathematical model

2.1. governing equations

The basic equations for two-dimensional compressible flow are the 2D Euler equations,

$$\mathbf{U}_t + \nabla \cdot \mathbf{F} = 0, \qquad \Omega \times (0,T) \tag{1}$$

where $\mathbf{U} = \left[\rho, \rho u, \rho v, E\right]^{\mathrm{T}}$, $\mathbf{F}_x = \left[\rho u, \rho u^2 + p, \rho uv, (E+p)u\right]^{\mathrm{T}}$, $\mathbf{F}_y = \left[\rho v, \rho uv, \rho v^2 + p, (E+p)v\right]^{\mathrm{T}}$, $\Omega \in R^2$, T is time variable, ρ is density, u and v are velocity component of x and y direction respectively, E is the total energy per unit volume, p is the pressure, and E is the total energy per unit volume

$$E = p/(\gamma - 1) + \rho\left(u^2 + v^2\right)/2 \tag{2}$$

where γ is the ratio of specific heat.

2.2. Level Set equation

We use the level set equation

$$\frac{\partial \varphi}{\partial t} + u\frac{\partial \varphi}{\partial x} + v\frac{\partial \varphi}{\partial y} = 0 \tag{3}$$

to keep track of the interface location as the zero level of φ. And φ is usually chosen as a sign distance function defined as followed

$$\varphi(x,y,0) = \begin{cases} > 0 & (x,y) \in \text{inside fluid 1} \\ = 0 & (x,y) \in \text{interface} \\ < 0 & (x,y) \in \text{outside fluid 1} \end{cases} \tag{4}$$

However, during its evolution, the level set function can lose the property of being the distance function[14]. So a re-initialized equation (5) is required to keep the function φ holding the characteristic of distance.

$$\frac{\partial \varphi(x,y,\tau)}{\partial \tau} + S(\varphi_0)\left(|\nabla \varphi| - 1\right) = 0 \tag{5}$$

where τ is fictitious time, $S(\varphi_0) = \varphi/\sqrt{\varphi^2 + \theta^2}$ is a sign function and $\theta = \min(\mathrm{d}x, \mathrm{d}y)$.

The Equation (3) is numerically solved using the third-order RK-TVD scheme for time discretization and the fifth-order WENO scheme[15] for space discretization. Re-initialized equation (5) is solved using fifth-order WENO scheme developed by Peng et al[15].

3. The implementation of the DG method

First, the equations (1) are discretized in space by using a DG method. $\forall t \in [0,T]$, the approximate solution $\mathbf{U}_h(\boldsymbol{X}, t)$ is sought in the finite element space of discontinuous functions

$$V_h = \left\{ v_h \in L^{\infty}(\Omega) : v_h|_K \in V(K), \forall K \in \Gamma_h \right\}$$

where Γ_h is a finite partition of the domain Ω, $V(K)$ is the so-called local space, which is taken as the collection of polynomials of degree k, for $k = 2$, in this paper and $\boldsymbol{X} = (x, y)$.

In order to determine the approximate solution $\mathbf{U}_h(\boldsymbol{X},t)$, we multiply Eq. (1) by a test function v and integrate over the element K. Then, the exact solution $\mathbf{U}(\boldsymbol{X},t)$ is replaced by approximation $\mathbf{U}_h(\boldsymbol{X},t)$, and the test function v is replaced by v_h. After applying the integration by part once, we recover the weak formulation form

$$\frac{\mathrm{d}}{\mathrm{d}t}\int_K \mathbf{U}_h(\boldsymbol{X},t)v_h\mathrm{d}\Omega+\sum_{e\in\partial K}\int_e \mathbf{F}(\mathbf{U}_h)\cdot\boldsymbol{n}_{e,K}v_h\mathrm{d}\Gamma-\int_K \mathbf{F}(\mathbf{U}_h)\cdot\nabla v_h\mathrm{d}\Omega=0 \tag{6}$$

where $\boldsymbol{n}_{e,K}$ denotes the outward unit normal to the edge *e*. Then, the flux $\mathbf{F}(\mathbf{U}_h)\cdot\boldsymbol{n}_{e,K}$ is replaced by the numerical flux $h^{e,K}(\boldsymbol{X},t)$, resulting in the scheme

$$\frac{\mathrm{d}}{\mathrm{d}t}\int_K \mathbf{U}_h(\boldsymbol{X},t)v_h\mathrm{d}\Omega+\sum_{e\in\partial K}\int_e h^{e,K}(\boldsymbol{X},t)v_h\mathrm{d}\Gamma-\int_K \mathbf{F}(\mathbf{U}_h)\cdot\nabla v_h\mathrm{d}\Omega=0 \tag{7}$$

The value of numerical flux, $h^{e,K}(\boldsymbol{X},t)$, at the point $(\boldsymbol{X},t)$ depends on two values of the approximate solution on $(\boldsymbol{X},t)$, one is obtained from the interior of element K, that is $\mathbf{U}_h\left(\boldsymbol{X}^{int(K)},t\right)=\lim_{y\to x,y\in K}\mathbf{U}_h(y,t)$, and the other is obtained from the exterior of the element K, that is $\mathbf{U}_h\left(\boldsymbol{X}^{ext(K)},t\right)=\begin{cases}\gamma_h(\boldsymbol{X},t) & \boldsymbol{X}\in\partial\Omega\\ \lim_{y\to x,y\notin K}\mathbf{U}_h(y,t) & \boldsymbol{X}\notin\partial\Omega\end{cases}$, where $\gamma_h(\boldsymbol{X},t)$ is the trace of the element.

Numerical flux is defined as $h^{e,K}(\boldsymbol{X},t)=h^{e,K}\left(\mathbf{U}_h\left(\boldsymbol{X}^{int(K)},t\right),\mathbf{U}_h\left(\boldsymbol{X}^{ext(K)},t\right)\right)$, which is a monotone flux for the scalar case and an exact or approximate Riemann solver for the system case. In this work, the simple Lax–Friedrichs flux is used, which is given as

$$h^{e,K}(a,b)=\frac{1}{2}\left[\boldsymbol{F}(a)\cdot\boldsymbol{n}_{e,K}+\boldsymbol{F}(b)\cdot\boldsymbol{n}_{e,K}-\alpha_{e,K}(b-a)\right] \tag{8}$$

Where $\alpha_{e,K}$ is the estimate of the largest eigenvalue of Jacobi matrix $(\partial/\partial\mathbf{U})\mathbf{F}(\mathbf{U}_h(\boldsymbol{X},t))\cdot\boldsymbol{n}_{e,K}$ on the interface of element. Furthermore, we replace the integrals by quadrature rules as

$$\int_e h^{e,K}(\boldsymbol{X},t)v_h(\boldsymbol{X})\mathrm{d}\Gamma\approx\sum_{l=1}^{L}\omega_l h^{e,K}(\boldsymbol{X}_{el},t)v_h(\boldsymbol{X}_{el})|e| \tag{9}$$

$$\int_K \mathbf{F}(\mathbf{U}_h(\boldsymbol{X},t))\cdot\nabla v_h(\boldsymbol{X})\mathrm{d}\Omega\approx\sum_{j=1}^{M}\underline{\omega}_j\mathbf{F}(\mathbf{U}_h(\boldsymbol{X}_{Kj},t))\cdot\nabla v_h(\boldsymbol{X}_{Kj})|K| \tag{10}$$

Substitute equation (9) and (10) into equation (7), finally we recover the weak expression

$$\frac{\mathrm{d}}{\mathrm{d}t}\int_K \mathbf{U}_h(\boldsymbol{X},t)v_h(\boldsymbol{X}_e)\mathrm{d}\Omega+\sum_{e\in\partial K}\sum_{l=1}^{L}\omega_l h^{e,K}(\boldsymbol{X}_{el},t)v_h(\boldsymbol{X}_{el})|e|-\sum_{j=1}^{M}\underline{\omega}_j\boldsymbol{F}(\boldsymbol{U}_h(\boldsymbol{X}_{Kj},t))\cdot\nabla v_h(\boldsymbol{X}_{Kj})|K|=0 \tag{11}$$

For convenient computation, the orthogonal basis functions $\{\phi_1,\phi_2,\cdots,\phi_j\}$ are used over the quadrilateral element K. Then, the expression for the approximate solution $\mathbf{U}_h(\boldsymbol{X},t)$ over the element K is taken as

$$\mathbf{U}_h(\boldsymbol{X},t)=\sum_{j=1}^{m}\hat{\mathbf{U}}_j(t)\phi_j \tag{12}$$

Let $v_h=\phi_i$ in (11), we obtain

$$\sum_j\frac{\mathrm{d}\hat{\mathbf{U}}_j}{\mathrm{d}t}\int_K\phi_j(\boldsymbol{X})\phi_i(\boldsymbol{X})\mathrm{d}\Omega+\sum_{e\in\partial K}\sum_{l=1}^{L}\omega_l h^{e,K}(\boldsymbol{X}_{el},t)\phi_i|e|-\sum_{j=1}^{M}\underline{\omega}_j\mathbf{F}(\mathbf{U}_{\mathbf{h}}(\boldsymbol{X}_{Kj},t))\cdot\nabla\phi_i|K|=0 \tag{13}$$

Let $\boldsymbol{M}_K$ is the mass matrix, for $\forall v_h\in V_h,\forall K\in\Gamma_h$, the formulation (12) can be rewritten in a concise ODEs form

$$\boldsymbol{M}_K \, \mathrm{d}\hat{\mathbf{U}}_h(t)/\mathrm{d}t = L_h\left(\hat{\mathbf{U}}_h(t), \gamma_h\right) \tag{14}$$

We discretize in time the above system of ODEs with Runge-Kutta method that is third-order accurate and the special steps as follows

1) Set $\hat{\mathbf{U}}_h^0 = P_{V_h}\left(\hat{\mathbf{U}}_0\right)$, the operator P_{V_h} is the L_2- projection into the finite element space V_h

2) for $n = 0, ..., N-1$ compute $\hat{\mathbf{U}}_h^{n+1}$ as follows:

a) Set $\hat{\mathbf{U}}_h^0 = \hat{\mathbf{U}}_h^n$,

b) for $i = 1, ..., k+1$, compute the intermediate functions

$$\hat{\mathbf{U}}_h^{(i)} = \left\{\sum_{l=0}^{i-1} \alpha_{il} \hat{\mathbf{U}}_h^{(l)} + \beta_{il} \Delta t^n L_h\left(\hat{\mathbf{U}}_h^{(l)}, \gamma_h\left(t^n + d_l \Delta t^n\right)\right)\right\}, \Delta t^n = t^{n+1} - t^n$$

c) Set $\hat{\mathbf{U}}_h^{n+1} = \hat{\mathbf{U}}_h^{k+1}$,

For more details on the value of α_{il}, β_{il} and d_l see Ref.6.

Under the high-order circumstances, in order to enhance the stability of the method and eliminate possible spurious oscillations in the approximate solution, a slope limiter is performed by the TVB corrected *minmod* function, which is introduced by Cockburn[6], as follows

$$\bar{m}(a_1, ..., a_m) = \begin{cases} a_1 & |a_1| \le M \Delta x^2 \\ s \min_i |a_i| & s = \mathrm{sign}(a_i) \\ 0 & \text{otherwise} \end{cases} \tag{15}$$

Where $M > 0$ is a constant, and more details of slope limiter see Ref.6.

4. GFM method on moving interfaces

A consistent numerical scheme is adopted in tradition for capturing shock waves in multi-media fluid simulation, but it is inevitable to introduce state variables of fluids at both interface sides and to cause non-physical oscillations. GFM[12] method is the single-phase flow calculation method to solve fluid one and fluid two, each flow is composed of real fluid on one interface side and Ghost fluid on the other interface side. This method uses interface intermittent relationship to keep pressure and the normal speed unchanged for those values across interface mesh, and only interpolate to entropy and tangential velocity, then uses these variables to compute the circulation across the interfaces, furthermore, the physical equation is solved.

Entropy and tangent velocity are extrapolated using the method in Ref.12. The partial differential equation extrapolated in normal direction is solved:

$$I_\tau \pm \boldsymbol{N} \cdot \nabla \varphi = 0 \tag{15}$$

where $\boldsymbol{N} = \nabla\varphi / |\nabla\varphi|$, is unit normal vector of mesh point. I is extrapolated variable such as entropy and tangent velocity. Fitting I in the region $\varphi > -\varepsilon$ with the value of I in the region $\varphi < -\varepsilon$ is expressed as symbol "+" keeping the real fluid value in the region $\varphi < -\varepsilon$ unchanged. Analogously, fitting I in the region $\varphi < \varepsilon$ with the value of I in the region $\varphi > \varepsilon$ is expressed as symbol "-" keeping the real fluid value in the region $\varphi > \varepsilon$ unchanged. In general, $\varepsilon = 1.5 \max(\Delta x, \Delta y)$.

5. Numerical results

In this section, two numerical test cases of two-media fluids are computed using DG level set method. Case one is a typically one dimensional sod shock-tube problem with initial state as

$$(\rho, u, v, p, \gamma)_L = (1.0, 0.0, 0.0, 1.0, 1.4), \ (\rho, u, v, p, \gamma)_R = (0.125, 0.0, 0.0, 0.1, 1.2)$$

The whole computational domain is [0:1] with 201 grid points and initial interface is located $x = 0.5$. The computed results including density, pressure, velocity and ratio of specific heats are plotted in Fig.1 at non-

dimensional time t=0.21, where circles represent exact cases and solid lines represent numerical solutions. We can easily see that the agreements between the numerical results and exact solutions are excellent.

Case two represents a Mach 1.22 air shock collapse of a helium bubble. The schematic for this problem are given in Fig. 2 with 321×81 grid points, where the upper and lower boundary conditions are a reflection for solid wall boundaries. The left and right boundary conditions are inflow and outflow respectively for the flow variables and linear extrapolation for level set function φ. The non-dimensionalized initial conditions are

$$(\rho,u,v,p,\gamma)=\begin{cases}(1,0,0,1,1.4) & \text{for pre-shocked air}\\ (1.3764,-0.394,0,1.5698,1.4) & \text{for post-shocked air}\\ (0.138,0,0,1,1.67) & \text{for helium bubble}\end{cases}$$

and the level set function $\varphi=-25+\sqrt{(x-175)^2+y^2}$, where $\varphi<0$ represents helium and $\varphi>0$ represents the air. Experimental results of this problem may be found in Ref.16. Very complex physics occurs in this problem especially after a re-entrant jet forms and impact the rear of the helium bubble.

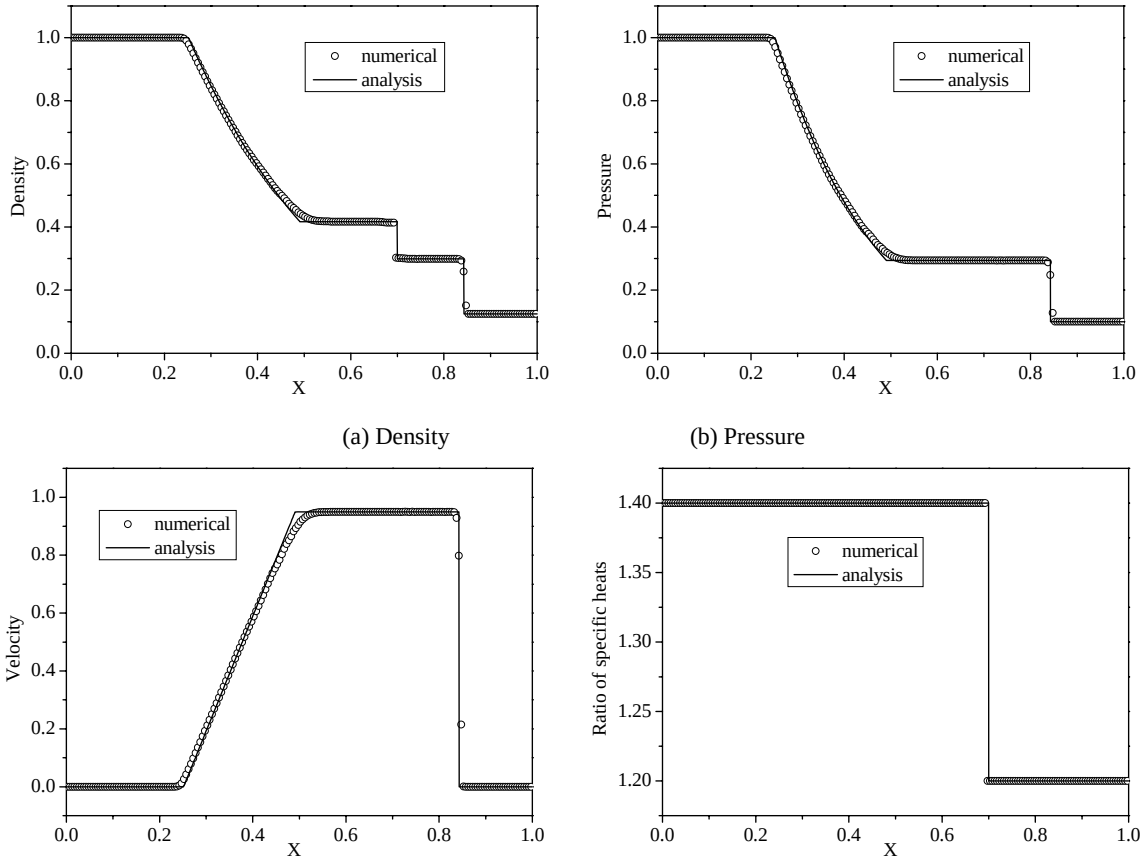

(a) Density (b) Pressure

(c) Velocity (d) Ratio of specific heats

Fig.1 Density, pressure, velocity and ratio of specific profile (t=0.21)

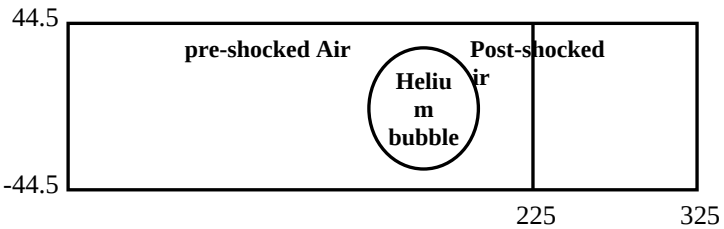

Fig 2 schematic diagram of shock wave passing helium bubble

Fig. 3 represents moving interface evolution at different dimensionless time. We can easily see that the right of the bubble is beginning to becomes flattened when the incident shock hits the bubble shown as in Fig. 3a at t=20. At the same time, the bubble moves left derived by shock and the right side becomes more flattened shown in Fig. 3b. With the time development, the right boundary becomes shrinking shown in Fig. 3c and eventually looks like a kidney at t=100 shown in Fig. 3d.

Fig.4 show fluid density contours at different non-dimensional time. When the incident shock hits the bubble, the incident shock is reflected from the bubble surface shown in Fig 4a. At the same time, the incident shock is partly transmitted inside the helium bubble and partly reflected from the bubble surface into the air shown in Fig. 4b. With the time development, the initial shock passed over the top of the bubble shown in Fig. 4c and interacts with the transmitted shock from the bubble shown in Fig. 4d. It is important to notice that the density contour shape in the bubble is the same as zero contour profile of level set function corresponding to the time, and the wave structures are similar as indicated by the experimental results[16].

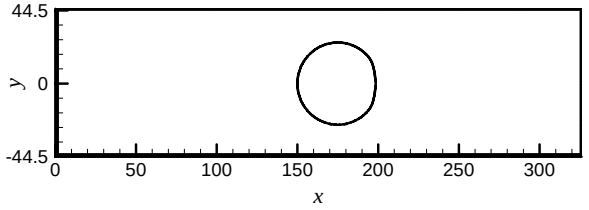

(a) t =20

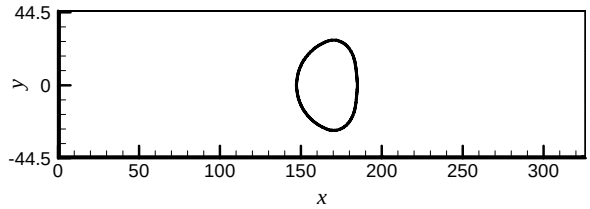

(b) t =40

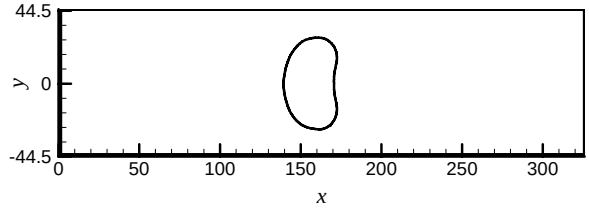

(c) t =60

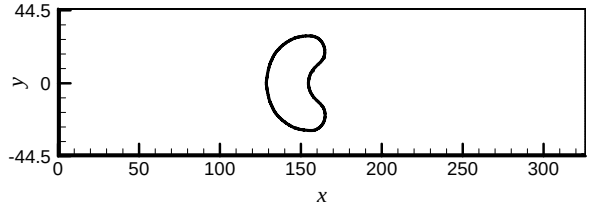

(d) t = 100

Fig.3 Moving interface evolution at differential time

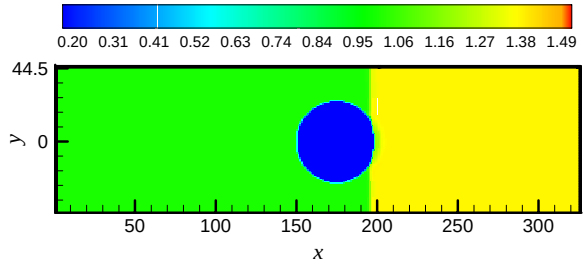

(a) t = 20

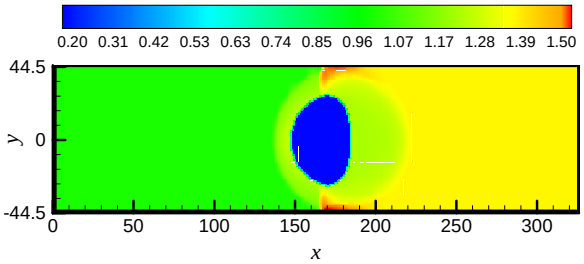

(b) t = 40

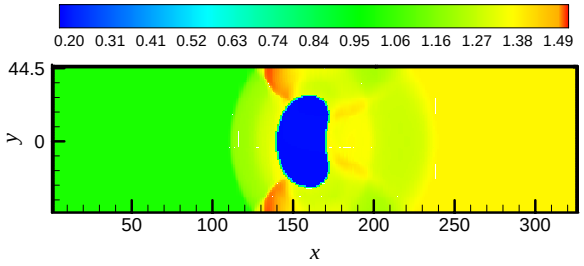

(c) t =60

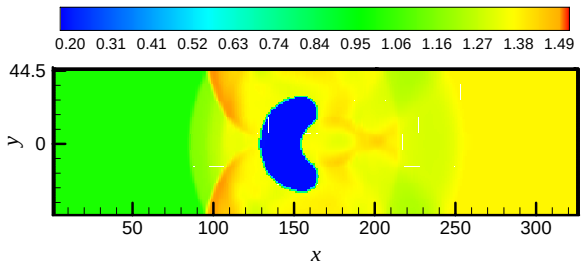

(d) t =100

Fig. 4 density contour at differential time

6. Conclusions

A DG method is developed to simulate two-media fluid flow. In computational, a level set method is used to capturing moving interfaces and a GFM with isobaric fix is used to disposing the interfaces boundary. Several test problems indicate that hardly nonphysical oscillations appear near the moving interface, which

illustrate the effectiveness of the method.

7. Acknowledgements

This work was supported by the National Natural Science Foundation of China (50976072), leading academic discipline project of Shanghai municipal education commission (J50501) and the science foundation for the excellent youth scholar of higher education of Shanghai (slg09003)

8. Reference

[1] W. H. Reed, T. R. Hill. Triangular Mesh Methods for the Neutron Transport Equation. *Scientific Laboratory Report*. Los Alamos, LA-UR-73-479, 1973.

[2] P. Lesaint, P. A. Raviart. On a Finite Element Method for Solving the Neutron Transport Equation. *Mathematical Aspects of Finite Elements in Partial Differential Equations*. Academic Press, San Diego, 1974.

[3] C. Johnson and J. Pitkaranta. An analysis of the Discontinuous Galerkin Method for a Scalar Hyperbolic Equation. *Math. Comput*. 1986, **46**(1).

[4] G. R. Richter. An Optimal-order Error Estimate for the Discontinuous Galerkin Method. *Math. Comput*. 1988, **50**: 75.

[5] T. Peterson. A Note on the Convergence of the Discontinuous Galerkin Method for a Scalar Hyperbolic Equation. *SIAM J. Numer. Anal*. 1991, **28**: 133.

[6] B. Cockburn, C. W. Shu, Runge-Kutta. Discontinuous Galerkin Methods for Convection-dominated Problems. *J. Sci. Comput*. 2001, **16**: 173-261.

[7] N. Chevaugeon, J. Xin and P. Hu. Discontinuous Galerkin Methods Applied to Shock and Blast Problems. *J. Sci. Comput*. 2005, **22**: 227-243.

[8] J. X. Qiu, B. C. Khoo and C. W. Shu. A Numerical Study for the Performance of the Runge Kutta Discontinuous Galerkin Method Based on Different Numerical Fluxes. *J. Comput. Phys*. 2006, **212**: 540-565.

[9] J. X. Qiu, T. G. Liu and B. C. Khoo. Simulations of Compressible Two-Medium Flow by Runge-Kutta Discontinuous Galerkin Methods with the Ghost Fluid Method. *Commun. Comput. Phys*. 2008, **3**: 479-504.

[10] J. Naber. A Numerical Solver for Compressure two-fluid Flow, Report MAS-E0505, CWI, http://oai.cwi.nl/oai/asset/10961/10961D.pdf, 2005.

[11] N. Robert, D. Nam, T. Theo. Direct Numerical Simulation of Compressible Multiphase Flows: Interaction of Shock Waves with Dispersed Multimaterial Media, ICMF'04, Yokohama, Japan, May 30-June 4 , 2004.

[12] R.P.Fedkiw, T.Aslam, B.Merriman, S.Osher. A Non-oscillatory Eulerian Approach to Interfaces in Multimaterial Flows(theGhost Fluid Method) [J]. *J. Comput. Phys*. 1999, **152**: 457-492.

[13] S. Osher, J. A. Sethian. Fronts propagating with curvature-dependent speed: algorithms based on Hamilton- Jacobi formulations. *J. comp. Phys*. 1988, **79**:12-49.

[14] S. Osher and R. P. Fedkiw. Level Set Methods: An Overview and Some Recent Results. *J. Comput. Phys*. 2001, **169**: 463-502.

[15] Jiang, G.S., and Peng, D.P. Weighted ENO schemes for Hamilton-Jacobi equations. *SIAM J. Sci. Comput*. 2000, **21**(6): 2126-2143.

[16] J. F. Haas and B. Sturtevant. Interactions of weak shock waves with cylindrical and spherical gas inhomogeneities. *J. Fluid Mech*. 1987, **181**: 41.